© 2019. Published by The Company of Biologists Ltd | Development (2019) 146, dev167452. doi:10.1242/dev.167452

RESEARCH ARTICLE

Common cellular origin and diverging developmental programs for different sesamoid bones

Shai Eyal, Sarah Rubin, Sharon Krief, Lihi Levin and Elazar Zelzer*

ABSTRACT

Sesamoid bones are small auxiliary bones that form near joints and contribute to their stability and function. Thus far, providing a comprehensive developmental model or classification system for this highly diverse group of bones has been challenging. Here, we compare our previously reported mechanisms of patella development in the mouse with those of two anatomically different sesamoids, namely lateral fabella and digit sesamoids. We show that all three types of sesamoid bones originate from *Sox9*$^{+}$/*Scx*$^{+}$ progenitors under the regulation of TGFβ and independently of mechanical stimuli from muscles. Whereas BMP2 regulates the growth of all examined sesamoids, the differentiation of lateral fabella or digit sesamoids is regulated redundantly by BMP4 and BMP2. Next, we show that whereas patella and digit sesamoids initially form in juxtaposition to long bones, lateral fabella forms independently and at a distance. Finally, our evidence suggests that, unlike the synovial joint that separates patella from femur, digit sesamoids detach from the phalanx by formation of a fibrocartilaginous joint. These findings highlight both common and divergent molecular and mechanical features of sesamoid bone development, which underscores their evolutionary plasticity.

KEY WORDS: Sesamoid bone, Joint, Sox9, Scleraxis, Tgfβ, BMP, Mouse

INTRODUCTION

Sesamoid bones constitute a special group of bones that are integral to the skeletons of many vertebrate species (Abdala et al., 2017; Bizarro, 1921; Corina Vera et al., 2015; Jerez et al., 2009; Maisano, 2002; Ponssa et al., 2010; Sarin et al., 1999). Estimated to have evolved 200 million years ago (Carter, 1998), sesamoid bones are usually small and flat with morphological resemblance to the sesame seed, hence their name (Vickaryous and Olson, 2007). In addition, sesamoid bones are typically embedded within tendons, notably in proximity to joints. However, despite these common characteristics, sesamoids vary tremendously in aspects such as location and penetrance both within and across species, and the type of joints they are associated with. This high degree of variability imposes a challenge on providing a comprehensive model for sesamoid bone development.

The patella, also known as the kneecap, is the largest sesamoid bone in mammals and is part of the patellofemoral joint, one of the two joints that compose the knee (Samuels et al., 2017). The patella is positioned within the patellar groove, which is located at the anterodistal part of the femur and is separated from it by the synovial patellofemoral joint. The patellar groove enables the patella to have a controlled slide during flexion and extension of the lower leg segment, whereas the synovial joint permits this high degree of flexibility while maintaining the integrity of the articular cartilage of the long bones that flank the synovial capsule (Schindler and Scott, 2011). The patella has a crucial effect on the stability and mechanics of the knee. It absorbs disruptive forces that are applied to the quadriceps tendon, within which it is embedded, and enhances the moment arm and resulting extension force of the quadriceps muscle (Bizarro, 1921; Lennox et al., 1994; Mottershead, 1988; Sarin et al., 1999; Sutton et al., 1976).

The smaller fabella is located opposite the patella at the back of the mammalian knee. Although it is similarly embedded within the lateral head tendon of the gastrocnemius muscle in both human and mouse, the attachment site of this tendon varies between the two species. In humans, the fabella is located behind the lateral condyle of the femur, whereas in mice it is found on its lateral side (Jin et al., 2017; Phukubye and Oyedele, 2011; Sarin et al., 1999). The fabella lacks articular cartilage and is, in addition, connected by the fabellofibular ligament to the fibular tip and to the proximolateral side of the meniscus by two separate bundles of fibers (Jin et al., 2017). These anatomical differences imply that, unlike patella, the function of the fabella is not to facilitate and enhance movement but rather restrict it by anchoring and stabilizing the knee, thus preventing possible external rotation of the tibia or hyperextension of the knee (Hauser et al., 2015).

In mice, digit sesamoids can be found in pairs at any metacarpo/metatarsophalangeal and proximal interphalangeal joints of any digit, at which they are dorsally embedded within the flexor digitorum tendon and anteriorly share articulation with the metacarpal/metatarsal bones. In contrast to the patella, they are unable to freely glide over these articulated joints, as they are physically connected to the proximal tip of the proximal phalanx by a fibrocartilaginous joint (Doherty et al., 2010). Thus, digit sesamoids serve as a guide for the long flexor tendons in directing and controlling the course of the strings during flexion of the digits (Wirtschafter and Tsujimura, 1961).

To date, the prevailing model for sesamoid development suggests that these bones are induced within the tendons that wrap around joints by mechanical forces that are generated by embryonic movement (Hall, 2005; Parsons, 1904). However, we recently reported that the patella forms by a different developmental mechanism (Eyal et al., 2015). Briefly, we demonstrated that the patella originates from chondroprogenitors that co-express both *Sox9* and scleraxis (*Scx*) and are distinct from the *Sox9*$^{+}$/*Scx*$^{-}$ chondroprogenitors that give rise to the long bone cartilaginous anlagen (Blitz et al., 2013; Eyal et al., 2015; Eyal et al., 2018 preprint). These progenitors form in juxtaposition to the femur and are later separated from it by the application of a joint formation

Weizmann Institute of Science, Department of Molecular Genetics, PO Box 26, Rehovot 76100, Israel.

*Author for correspondence (eli.zelzer@weizmann.ac.il)

S.E., 0000-0001-8131-8077; E.Z., 0000-0002-1584-6602

Received 7 May 2018; Accepted 1 February 2019

Development (2019) 146, dev167452. doi:10.1242/dev.167452

program. TGFβ and BMP4 signaling pathways were shown to be required for patella precursor specification and differentiation, respectively. Finally, we found that mechanical load is not necessary for patella formation, but is needed for its separation from the femur by regulating the formation of the patellofemoral joint. Although our findings pertain specifically to patella formation, they raise the question of whether our model for patella development could be applied to other sesamoid bones.

In this study, we test our model of patella development on the development of the fabella and digit sesamoids, which, as mentioned, are different from the patella in their anatomical, histological and functional properties. We show that all examined sesamoid bones originated from *Sox9*$^{+}$/*Scx*$^{+}$ progenitors that were induced independently of mechanical stimuli. We further show that these progenitors require TGFβ signaling for their specification, BMP2 signaling for their growth, and redundant interaction between BMP4 and BMP2 signaling for their differentiation. We provide evidence that suggests the sesamoids may develop away from the skeleton, or separate from the bone shaft through mechanical load-dependent formation of a synovial joint, or through mechanical load-independent formation of a fibrocartilaginous joint.

RESULTS

Sox9^{+}/*Scx*$^{+}$ chondroprogenitors give rise to sesamoid bones

Previously, we described a mechanism for patella development (Eyal et al., 2015). To investigate the generality of this mechanism, we analyzed comparatively development of the patella with that of two other subgroups of sesamoid bones, namely the lateral fabella and the metacarpophalangeal sesamoids. The two are similar to the patella in their full penetrance in both human and mice, but are dissimilar from it in their anatomy, histology and functions. We first compared the anatomy of the three sesamoid bones in mice using both micro-CT scans and histological sections (Fig. 1). Our results showed that, by E18.5, all sesamoid bones have formed and were embedded within tendons. The patella, which was separated from the femur by the patellofemoral synovial joint on its dorsal side, was ventrally embedded within the quadriceps tendon (Fig. 1A,Ci,Cii). The lateral fabella was embedded within the tendon of the lateral head of the gastrocnemius muscle, which attaches the dorsolateral condyle of the femur, and connected at its base to the lateral meniscus by the fabellofibular ligament (Fig. 1A,Di,Dii). The third metacarpophalangeal sesamoid bone (III-MCPS) was separated from the metacarpal bone by synovial space on its ventral aspect and embedded within the flexor digitorum tendon on its proximodorsal aspect (Fig. 1A,Ei,Eii). Micro-CT imaging showed that the III-MCPS was distinct from the proximal phalanx; yet, histologically we observed an unfamiliar tissue that connected the III-MCPS and the posterior tip of the proximal phalanx (Fig. 1Eii; enlarged boxed area), most likely the primordium of the fibrocartilage tissue that connects the metacarpophalangeal sesamoid bone to the proximal phalanx in adult mice (Doherty et al., 2010).

Patella precursors, which co-express *Sox9* and *Scx*, are added secondarily to the *Sox9*$^{+}$/*Col2a1*$^{+}$ chondrocytes of the femur anlage (Eyal et al., 2015). To examine whether the lateral fabella and III-MCPS originated from similar progenitors, we first sought to find the developmental stage at which these sesamoids start to form. For that, we harvested and sectioned embryonic wild-type (WT) knees or carpal digits at sequential developmental stages from E13.5 to E17.5 and immunostained them using antibodies for SOX9, a marker for chondroprogenitors, and COL2A1, a marker for

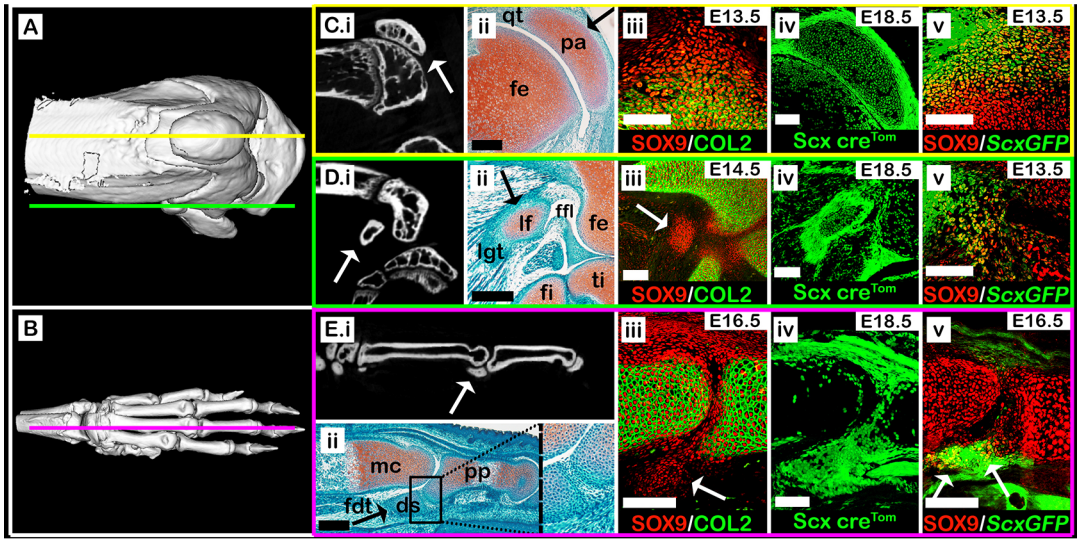

Fig. 1. Sesamoid bones arise from *Sox9*$^{+}$/*Scx*$^{+}$ progenitors. (A,B) Micro-CT scans of an adult knee (A) and forelimb autopod (B). Yellow line (A) indicates sagittal sections through the patella, as shown in panels Ci-Cv, green line (A) indicates sections through the lateral fabella, as shown in panels Di-Dv, and pink line (B) indicates sections through the digit sesamoid, as shown in panels Ei-Ev. (Ci-Ei) Selected sagittal planes from micro-CT scans of both knee and autopod. White arrows indicate sesamoid bones. (Cii-Eii) Sagittal sections through limbs of E17.5 WT embryos stained by Safranin-O. Black arrows indicate sesamoid bones. Cii shows that the patella is embedded within the quadriceps tendon. Dii shows that the lateral fabella is embedded within the lateral gastrocnemius tendon. Eii shows that the digit sesamoid is embedded within the flexor digitorum tendon and connected to the proximal phalanx by a fibrocartilage tissue (boxed area, enlarged on right). (Ciii-Eiii) Sagittal sections through limbs of WT embryos immunostained against SOX9 and COL2A1 show that sesamoid bones are formed at different developmental stages after the differentiation of the long bone cartilaginous anlagen (white arrows). Note the specification of patella and digit sesamoid precursors in continuum with the bone shaft anlagen. (Civ-Eiv) Sagittal sections through E18.5 limbs from *Scx-Cre*^{tdTomato} embryos indicate that all three sesamoid bones were formed by precursor cells that descended from *Scx*-expressing cells. (Cv-Ev) Sagittal sections through limbs of *ScxGFP* embryos stained against SOX9 show that all three sesamoid bones are formed by *Sox9*$^{+}$/*Scx*$^{+}$ progenitors (white arrows). ds, digit sesamoid; fdt, flexor digitorum tendon; fe, femur; ffl, fabellofibular ligament; fi, fibula; lf, lateral fabella; lgt, lateral gastrocnemius tendon; mc, metacarpal bone; pa, patella; pp, proximal phalanx; qt, quadriceps tendon; ti, tibia. Scale bars: 200 µm (Cii-Eii); 100 µm (Ciii-Ev).

Development (2019) 146, dev167452. doi:10.1242/dev.167452

chondrocytes. At E14.5, *Sox9*$^{+}$/*Col2a1*$^{-}$ cells marked the undifferentiated lateral fabella precursors, whereas *Sox9*$^{+}$/*Col2a1*$^{+}$ differentiated chondrocytes marked the femur and tibia (Fig. 1Diii). Notably, whereas the *Sox9*$^{+}$/*Col2a1*$^{-}$ patella precursors developed in juxtaposition to the femur, lateral fabella precursors were not connected to either femur or tibia (Fig. 1Ciii,Diii).

The *Sox9*$^{+}$/*Col2a1*$^{-}$ III-MCPS precursors were first observed at E16.5, subsequent to the differentiation of both metacarpal and proximal phalanx anlagen. Interestingly, at that stage, these precursors extended continuously from the proximodorsal aspect of the proximal phalanx (Fig. 1Eiii). This implies that later in development, they will have to detach from the proximal phalanx, similar to the process seen in the patella (Eyal et al., 2015).

Having established the initiation stage of these sesamoids, we next examined their cellular origin. For that, we performed a lineage tracing experiment using the *Scx-Cre* driver mouse crossed with tdTomato reporter mouse. We observed in sagittal sections of E18.5 knees and forelimb digits that patella, lateral fabella and III-MCPS cells were of *Scx*$^{+}$ lineage (Fig. 1Civ,Div,Eiv). Next, we confirmed that, as seen in patella progenitors, both lateral fabella and III-MCPS progenitor cells co-expressed *Sox9* and *Scx*. For that, sectioned knees and carpal digits of transgenic *ScxGFP* embryos were immunostained for SOX9 to highlight chondrocytes and, specifically, *Sox9*$^{+}$/*Scx*$^{+}$ chondroprogenitors. We observed large populations of *Sox9*$^{+}$/*Scx*$^{+}$ chondroprogenitors at the presumptive sites of patella, lateral fabella and III-MCPS formation (Fig. 1Cv, Dv,Ev). Collectively, these results confirmed that both lateral fabella and III-MCPS precursors formed in accordance to the patella model, namely from *Sox9*$^{+}$/*Scx*$^{+}$ chondroprogenitors that formed following differentiation of the long bone primordium cells.

Initiation of sesamoid bones is independent of mechanical load

Sesamoid bone development has been assumed to be induced by mechanical signals that are produced by embryonic movement (Parsons, 1904; Parsons, 1908). Yet, we have reported that patella induction was mechanical load-independent (Eyal et al., 2015). We therefore re-examined the paradigm of mechanical load-dependent induction of sesamoid bones by studying the formation of lateral fabella and III-MCPS in paralyzed homozygous *mdg* mutant embryos; heterozygous *mdg* embryos were used as controls (Pai, 1965). Examination of histological sections through knees and carpal bones of E17.5 mutants showed, as was previously described, that the patella was developing (Fig. 2A,A′). Similarly, we observed that both lateral fabella and III-MCPS were formed in the mutant as well (Fig. 2B-C′). These results provide conclusive support for our model by indicating that the induction of sesamoid bone formation is independent from muscle-induced mechanical load.

TGFβ and BMP signaling regulate sesamoid bone development

Another feature of patella development is the regulation of its *Sox9*$^{+}$/*Scx*$^{+}$ precursors by both TGFβ and BMP4 signaling pathways (Eyal et al., 2015). Having identified a similar cellular origin, we proceeded to examine the involvement of these pathways in lateral fabella and III-MCPS development. In addition, we examined the involvement of *Bmp2*, a paralog of *Bmp4* (Gamer et al., 2018; Pignatti et al., 2014). For that, *Tgfbr2*, *Bmp4* or *Bmp2* were specifically knocked out (cKO) from early limb mesenchyme using *Prx1-Cre* as a deleter mouse (*Prx1-TgfβRII*^{floxed}; *Prx1-Bmp4*^{floxed}; *Prx1-Bmp2*^{floxed}) (Chytil et al., 2002; Liu et al., 2004; Logan et al., 2002; Ma and Martin, 2005; Selever et al., 2004); *Prx1-Cre*-negative embryos were used as controls. Then, sections through the knees and digit bones of E17.5 mutant and control embryos were stained using Safranin-O (Fig. 3A-F″). Our examination revealed that similar to patella, both lateral fabella and III-MCPS were completely absent in *Prx1-TgfβRII*^{floxed} mutants (Fig. 3A-B″). Focusing on the BMP pathways, we found that in contrast to our previous findings for patella formation (Eyal et al., 2015), loss of *Bmp4* in limb mesenchyme had no effect on the formation of lateral fabella and III-MCPS (Fig. 3C-D″). Similarly, examination of the *Prx1-Bmp2*^{floxed} mutants revealed that all sesamoids were formed; however, all displayed growth retardation (Fig. 3E-F″).

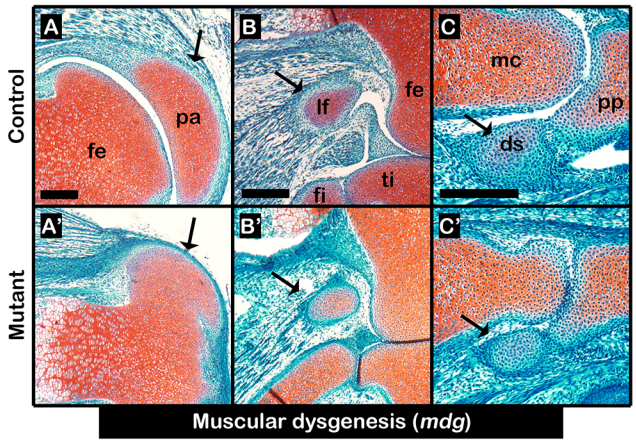

Fig. 2. Initiation of sesamoid bone formation is independent of mechanical stimuli. (A-C′) Sagittal sections through E17.5 limbs from control heterozygous *mdg* embryos (A-C) and homozygous *mdg* mutant (A′-C′) embryos stained by Safranin-O show that mechanical load is not needed for sesamoid bone initiation or growth, nor for fibrocartilage joint formation between digit sesamoid and proximal phalanx; however, it was needed for patellofemoral joint formation. Black arrows indicate sesamoid bones. ds, digit sesamoid; fe, femur; fi, fibula; lf, lateral fabella; mc, metacarpal bone; pa, patella; pp, proximal phalanx; ti, tibia. Scale bars: 200 µm.

Our finding that the exclusive loss of either *Bmp2* or *Bmp4* did not abolish the formation of lateral fabella and III-MCPS raised the possibility that these BMPs have a redundant function (Bandyopadhyay et al., 2006). To study this hypothesis, we crossed *Prx1-Bmp2*^{floxed}; *Bmp4*$^{floxed/+}$ mice *with Prx1-Bmp2*^{floxed}; *Bmp4*^{floxed} mice to generate mutant embryos that lack both *Bmp2* and *Bmp4* in limb mesenchyme; *Prx1-Cre*-negative embryos were used as controls. As seen in Fig. 3G-H″, the loss of a single copy of *Bmp4* allele on the background of a homozygous *Prx1-Bmp2*^{floxed} mutation resulted in fabella aplasia, whereas *Prx1-Bmp2*^{floxed}; *Bmp4*^{floxed} double cKO resulted in aplasia of all three sesamoid bones that were examined (Fig. 3I-J″). Collectively, these results suggest that sesamoid bones are regulated by both TGFβ and BMP signaling.

The metacarpophalangeal sesamoids are separated from the phalanx tip by formation of a fibrocartilaginous joint

Although digit sesamoids are distinct from the proximal phalanx in neonatal mice, at E16.5 the III-MCPS precursors appeared to be continuous with the cartilage anlage of the proximal phalanx (Fig. 1Eiii). By E18.5, these precursors were detached from the proximal phalanx, although they remained connected to it by a fibrocartilage-like tissue (Fig. 1Eii). To date, little is known about the mechanisms that underlie the genesis of the fibrocartilaginous joint. To study the origin of the fibrocartilage joint cells, we performed lineage tracing experiments using either *Scx-Cre* or

Development (2019) 146, dev167452. doi:10.1242/dev.167452

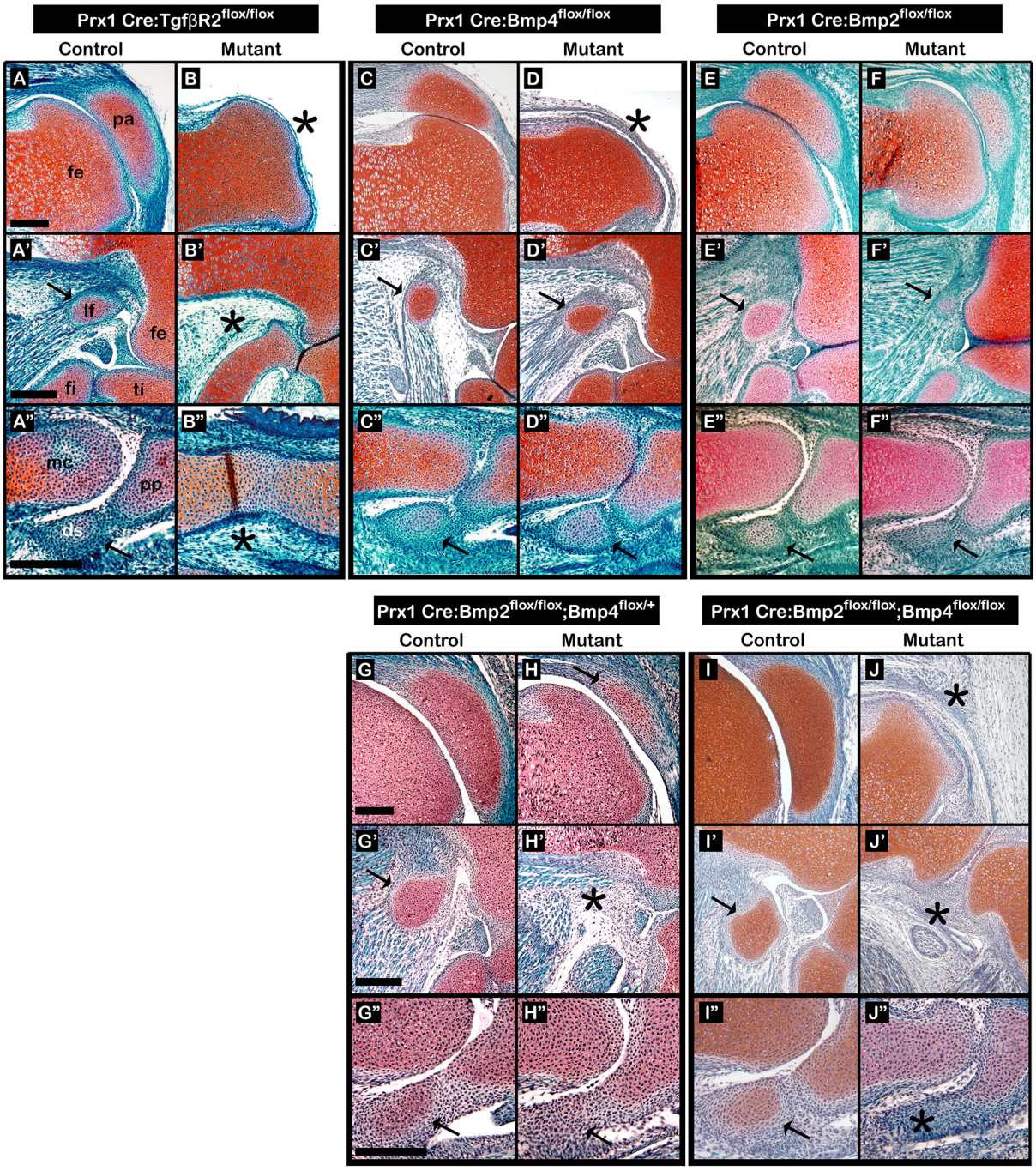

Fig. 3. TGFβ signaling regulates initiation of all sesamoid bones, whereas BMP signaling has varying regulatory roles. (A-J″) Sagittal sections through limbs from E17.5 *Prx1-TgfβRII*^{floxed} (A-B″), *Prx1-Bmp4*^{floxed} (C-D″) and *Prx1-Bmp2*^{floxed} (E-F″) mutants, and from E18.5 *Prx1-Bmp2*^{floxed}*;Bmp4*$^{floxed/+}$ (G-H″) and *Prx1-Bmp2*^{floxed}*;Bmp4*^{floxed} (I-J″) mutants. *Prx1*-Cre-negative embryos were used as controls. All samples were stained by Safranin-O. Limb-specific ablation of TGFβ signaling resulted in sesamoid bone aplasia (A-B″). Limb-specific ablation of *Bmp4* resulted in patellar aplasia, whereas both lateral fabella and III-MCPS appear to be unaffected (C-D″). Limb-specific ablation of *Bmp2* did not affect sesamoid bone initiation, yet resulted in sesamoid bone hypoplasia (E-F″). Limb-specific ablation of *Bmp2* and one allele of *Bmp4* resulted in sesamoid bone hypoplasia and fabella aplasia (G-H″). Limb-specific ablation of both *Bmp2* and *Bmp4* resulted in complete arrest of sesamoid bones initiation (I-J″). Black arrows indicate sesamoid bones; black asterisks indicate missing sesamoid bones. Abbreviations: ds, digit sesamoid; fe, femur; fi, fibula; lf, lateral fabella; mc, metacarpal bone; pa, patella; pp, proximal phalanx; ti, tibia. Scale bars: 200 µm.

Sox9-CreER^{T2} driver mice crossed with tdTomato reporter mice. As seen in sagittal sections of E18.5 forelimb digits of *Scx-Cre: tdTomato* embryos, the fibrocartilage joint cells were all *Scx*$^{+}$ (Fig. 4A). In parallel, sagittal sections of E18.5 forelimb digits of *Sox9-CreER*^{T2}*: tdTomato* embryos, to which tamoxifen was administered at E13.5, showed positive labeling of the fibrocartilage joint cells (Fig. 4B). Labeling of the fibrocartilage joint cells by both *Scx-Cre: tdTomato* and *Sox9-CreER*^{T2}*: tdTomato* suggests that these joint cells are descendant of *Sox9*$^{+}$/*Scx*$^{+}$ progenitors.

To further characterize molecularly the process of fibrocartilage joint formation, we performed double-fluorescent *in situ* hybridization using probes for cartilage marker *Sox9*, tendon cell markers *Scx* and

Development (2019) 146, dev167452. doi:10.1242/dev.167452

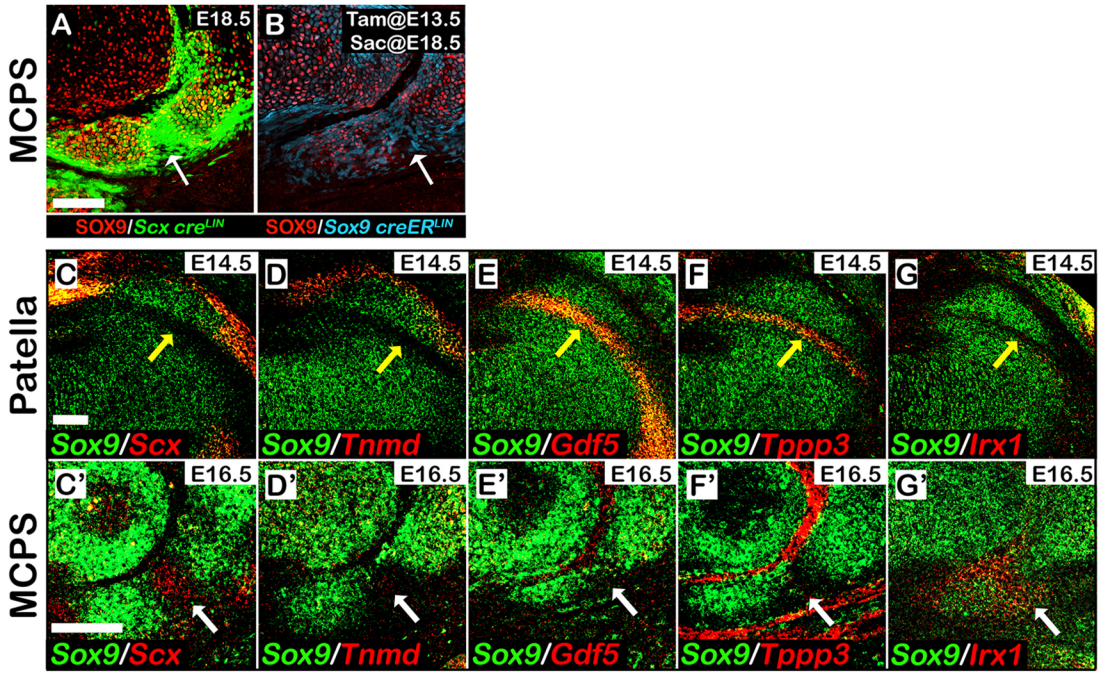

Fig. 4. Lineage tracing and gene expression analyses of cells that form the fibrocartilaginous joint that separates the metacarpophalangeal sesamoid from the proximal phalanx. (A,B) Sagittal sections through E18.5 digits from *Scx-Cre: tdTomato* (A) and *Sox9-CreER^{T2}: tdTomato* (B) embryos co-stained using SOX9 antibody. Induction of *Cre* recombinase by tamoxifen was at E13.5 (B). Tracing of both *Scx-Cre: tdTomato* and induced *Sox9-CreER^{T2}: tdTomato* lineages suggested that the fibrocartilage joint cells are descendants of the III-MCPS *Sox9$^+$/Scx$^+$* progenitors. White arrows indicate the connecting fibrocartilage tissue. (C-G′) Sagittal sections through E14.5 knees (C-G) or E16.5 digits (C′-G′) from WT embryos analyzed using dbFISH using DIG- and FITC-labeled antisense RNA probes for *Sox9* and either *Scx* (C), *Tnmd* (D), *Gdf5* (E), *Tppp3* (F) or *Irx1* (G). The patella is ventrally embedded within the quadriceps tendon, marked by *Scx* and *Tnmd* expression (C,D), and separated dorsally by the patellofemoral synovial joint, marked by *Gdf5* and *Tppp3* expression (E,F). Yellow arrows indicate the patellofemoral synovial joint. In contrast, III-MCPS is neither connected to the proximal phalanx by a tendon nor separated from it by a synovial joint, as indicated by the absence of *Tnmd* (D′), *Gdf5* (E′) and *Tppp3* (F′) expression at the connecting fibrocartilage tissue (marked by white arrows). Analysis of *Irx1* expression indicates that, whereas *Irx1* is highly expressed in the fibrocartilage tissue (G′), it is completely absent from the patellofemoral synovial joint region (G). Scale bars: 100 µm.

Tnmd, and joint-forming cell markers *Gdf5* and *Tppp3*. As has been previously reported, *Scx* and *Tnmd* expressions were observed within the tendon that envelops the patella on its ventral aspect, whereas *Gdf5* and *Tppp3* were expressed within the forming patellofemoral joint (Fig. 4C-F). However, within the tissue that connects the metacarpophalangeal sesamoid bone and the proximal phalanx, *Scx* expression was observed (Fig. 4C′), whereas expression of *Tnmd*, *Gdf5* or *Tppp3* could not be detected (Fig. 4D′-F′).

Recently, Iroquois genes *irx5a* and *irx7* were shown to mark the forming cartilaginous hyoid joint in the zebrafish (Askary et al., 2015), whereas *Irx1* was reported to be highly expressed within the digit joints in mice (McDonald et al., 2010). We therefore examined the involvement of Irx genes in sesamoid bone development. For that, we performed double-fluorescent *in situ* hybridization using complementary RNA probes against *Sox9* and *Irx1*. As seen in Fig. 4G′, *Irx1* was specifically expressed within the connecting tissue between the metacarpophalangeal sesamoid bone and the proximal phalanx, but was excluded from other joint compartments in the digits and from the patellofemoral synovial joint (Fig. 4G,G′). The combined expression of *Irx1* and *Scx* and the absence of *Tnmd* in the connective tissue between the metacarpophalangeal sesamoid bone and the proximal phalanx suggest that *Irx1* and *Scx* can serve as markers for fibrocartilaginous joint.

DISCUSSION

Sesamoid bones are small auxiliary bones that are highly variant in positioning, size and number (Bizarro, 1921; Jerez et al., 2009; Pearson and Davin, 1921b; Ponssa et al., 2010; Sarin et al., 1999). To date, the mechanism that regulates the development of these bones and allows the variations among them is unknown. Here, by comparing the development of three different sesamoid bones, namely patella, lateral fabella and III-MCPS, we identify common molecular and cellular mechanisms that underlie these processes. Interestingly, we also identify points of diversion in their developmental program, which could provide a mechanistic explanation to the variability within this family of bones (Fig. 5).

Our finding that all three studied sesamoid bones originated in *Sox9$^+$* and *Scx$^+$* precursors is interesting, because this lineage also contributes to the formation of bone superstructures, protrusions that project from the long bone surface and serve as attachment sites for tendons (Blitz et al., 2009; Blitz et al., 2013). These observations led us to suggest that bone superstructures and sesamoid bones can be placed under one category. Nevertheless, whereas bone superstructures protrude from the long bone shaft, sesamoid bones are auxiliary to it. Our finding that both patella and III-MCPS are separated from their bone of origin by a joint formation process offers a strategy for transforming a bone superstructure into a sesamoid bone, namely by detachment. Another way to determine between the development of a bone superstructure or a sesamoid bone is by regulating the spatial distribution of *Sox9$^+$/Scx$^+$* precursors. If the condensation of the *Sox9$^+$/Scx$^+$* precursors is adjacent to the target bone, then a bone superstructure will develop, as in the case of the deltoid tuberosity (Blitz et al., 2013; Sugimoto et al., 2013). Conversely, if these cells condense away from the target bone, a sesamoid bone will be formed, as in the case of the lateral fabella (Fig. 5).

Development (2019) 146, dev167452. doi:10.1242/dev.167452

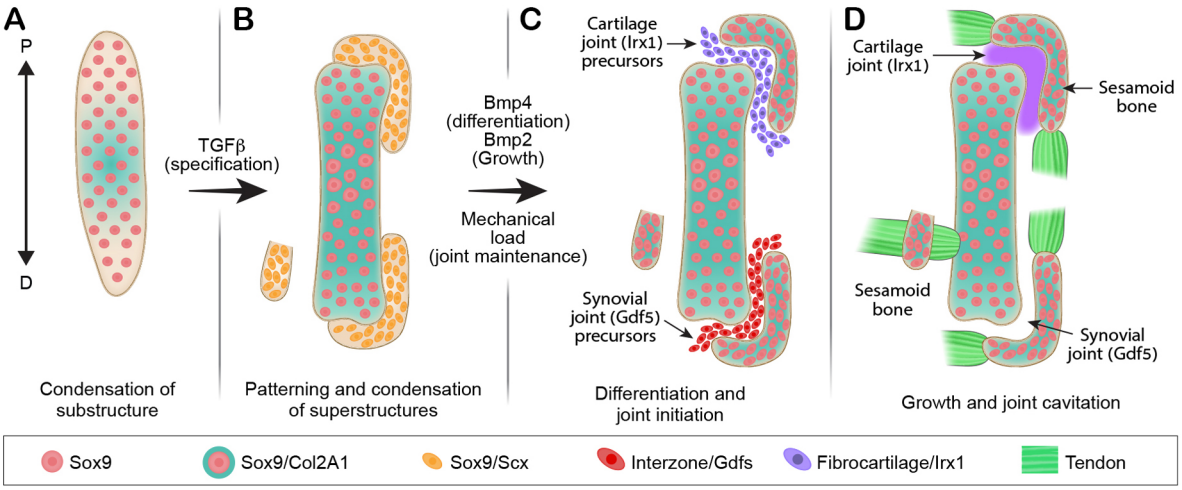

Fig. 5. Molecular and mechanical signals facilitate development and anatomical variation of sesamoid bones. (A,B) We propose that secondary pools of *Sox9* and *Scx* co-expressing progenitor cells are specified in proximity to the primary *Sox9*$^{+}$ cartilaginous anlagen. These cells are regulated by TGFβ and BMP4 that are required for their specification and differentiation, whereas BMP2 signaling is required for sesamoid bone growth. (C,D) After differentiation, some of these modules become bone eminences that are integral to the skeletal substructure and serve as attachment sites for tendons, whereas others develop away from it and form a sesamoid bone. However, under different environmental conditions and pressures, attached modules can be separated from the cartilage anlage by formation of a joint between them. This leaves the module superficially embedded within the tendon, thus creating a sesamoid bone. D, distal; P, proximal.

An example for such transitional plasticity between sesamoid bones and superstructures is given by olecranon development. In mammals, the olecranon forms as a bone superstructure at the proximal tip of the ulna, whereas in some anurans (frogs) it develops as a detached patella-like sesamoid bone (Ponssa et al., 2010), accordingly dubbed patella ulnaris. Presumably, formation of the olecranon as a sesamoid bone in earlier vertebrates preceded its formation as a fused superstructure in mammals. Interestingly, studies in several mutated mouse lines have also demonstrated this developmental plasticity. Compound *Hox11*^{aadd} mutant embryos were shown to exhibit a detached olecranon, similar to the patella ulnaris of anurans (Koyama et al., 2010). Another example was given by homozygous *Pbx1* mutant embryos, which developed a detached sesamoid-like deltoid tuberosity (Selleri et al., 2001).

The detachment mechanism was hypothesized a century ago by Pearson and Davin (1921a, b), who suggested that sesamoid bones originate from existing bone eminences that detached from long bone shafts. F. G. Parsons proposed a contrary hypothesis, suggesting that sesamoid bones develop independently yet could, in some cases, attach to neighboring long bones and become a bony eminence (Parsons, 1904; Parsons, 1908). Our data reconcile between these two opposing models by placing both bone eminences and sesamoid bones under one category of cartilage elements that develop from secondary *Sox9*$^{+}$/*Scx*$^{+}$ chondroprogenitors. Moreover, they share a molecular regulation mechanism, as both require TGFβ/BMP signaling for their development (Blitz et al., 2013; Eyal et al., 2015).

Interestingly, our findings also suggest that both genetic and mechanical regulation are involved in facilitating developmental diversity, as indicated by both global and specific genetic regulation of the TGFβ/BMP signaling pathways and by the requirement of mechanical stimuli for patellofemoral joint formation. Our results show that TGFβ signaling is necessary for the formation of all three sesamoids. Moreover, we show that BMP2 and BMP4 are redundantly necessary for sesamoid bone formation. Interestingly, however, whereas BMP2 signaling regulated the growth of all three bones, BMP4 specifically regulated differentiation of patella progenitors.

Another example for the diversity in the regulation of sesamoid bone development is the involvement of mechanical signals. First, we found no effect for lack of these signals on the formation of the lateral fabella. Similarly, the III-MCPS was formed and separated by the formation of a fibrocartilaginous joint in the absence of mechanical signaling. Yet, as we have previously shown, patella separation through the formation of a synovial joint is mechanical load-dependent (Eyal et al., 2015). In addition to the difference in mechanosensitivity, cells at the presumptive site of the developing fibrocartilaginous joint displayed a distinct expression profile compared with that of developing synovial joints. They expressed the tendon marker *Scx* and joint marker *Irx1*, but failed to express other markers such as *Tnmd*, *Gdf5* or *Tppp3*. These findings shed light on the little known process of fibrocartilaginous joint formation.

Altogether, these variations in the developmental programs of the different sesamoid bones may provide an initial explanation for the diversity in anatomy and function of this unique group of bones.

To conclude, our results provide further insight into the origin, formation and development of sesamoid bones. We suggest that these bony elements originate from pools of *Sox9*$^{+}$/*Scx*$^{+}$ chondroprogenitors. We further show that some sesamoid bones form initially in juxtaposition to the long bone anlagen and are later separated by different programs of joint development. In contrast, we show that other sesamoids, such as the lateral fabella, can form as a separate entity. Finally, we demonstrate that a combination of genetic and mechanical regulatory programs is applied to achieve anatomical and ultimately functional variation during sesamoid bone development.

MATERIALS AND METHODS

Animals

All experiments involving mice were approved by the Institutional Animal Care and Use Committee (IACUC) of the Weizmann Institute. For all timed pregnancies, plug date was defined as E0.5. For harvesting of embryos, timed-pregnant females were euthanized by cervical dislocation. The gravid uterus was dissected out and suspended in a bath of ice-cold

Development (2019) 146, dev167452. doi:10.1242/dev.167452

phosphate-buffered saline (PBS) and the embryos were harvested after removal of the placenta. Tail genomic DNA was used for genotyping by PCR. All experiments were performed in at least three biological repeats (i.e. three embryos from three separate litters).

Mice that were heterozygous for the mutation muscular dysgenesis (*mdg*) (Pai, 1965) were kindly provided by G. Kern (Innsbruck Medical University, Austria). *Scx-Cre* and *ScxGFP* transgenic mice were obtained from R. Schweitzer (Shriners Hospital for Children Research Division, Portland, OR, USA) and R. L. Johnson (The University of Texas MD Anderson Cancer Center, Houston, TX, USA). *Sox9-CreER^{T2}* mice (Soeda et al., 2010) were kindly provided by the laboratory of Haruhiko Akiyama (Kyoto University, Japan). C57/Bl6 mice (The Jackson Laboratory) were used for micro-CT analyses.

The generation of *Prx1-Cre* (Logan et al., 2002), floxed-*Tgfbr2* (Chytil et al., 2002), floxed-*Bmp4* (Liu et al., 2004; Selever et al., 2004), floxed-*Bmp2* (Ma and Martin, 2005), *ScxGFP* (Pryce et al., 2007), *Sox9-CreER^{T2}* (Soeda et al., 2010) and *Rosa26-tdTomato* (Madisen et al., 2010) mice have been described previously. To create *mdg* mutant mice, animals heterozygous for the mutation were crossed; heterozygous *mdg* embryos were used as a control. To create *Prx1-Tgfbr2*, *Prx1-Bmp4* or *Prx1-Bmp2* mutant mice, floxed-*Tgfbr2*, floxed-*Bmp4* or floxed-*Bmp2* mice were mated with *Prx1-Cre-Tgfbr2*, *Prx1-Cre-Bmp4* or *Prx1-Cre-Bmp2* mice, respectively. To create compound *Prx1-Bmp2;Bmp4* mutant mice, floxed-*Bmp2;Bmp4* mice were mated with *Prx1-Cre-Bmp2;Bmp4* mice. As a control, *Prx1-Cre*-negative embryos were used. For genetic lineage tracing analysis, *Scx-Cre* or *Sox9-CreER^{T2}* mice were crossed with homozygous *Rosa26-tdTomato* mice. Induction of *Cre* recombinase was performed at various pregnancy stages by administration of 0.03 mg/g tamoxifen/body weight in corn oil by oral gavage (stock concentration was 5 mg/ml).

Ex vivo micro-CT scanning

Before scanning, limbs of postnatal day (P) 14 C57/Bl6 mice (Jackson) were dissected, fixed overnight in 4% paraformaldehyde (PFA)/PBS and dehydrated in an ethanol series to 100%. Samples were then scanned *ex vivo* in 100% ethanol using the Xradia MicroXCT-400 (Zeiss) at 30 kV and 4.5 W or 40 kV and 8 W.

Paraffin sections

For preparation of paraffin sections, embryos were harvested at various ages, dissected and fixed in 4% PFA/PBS at 4°C overnight. After fixation, tissues were dehydrated in an ethanol series to 100% and embedded in paraffin. The embedded tissues were sectioned at 7 µm and mounted onto slides.

OCT-embedded sections

For preparation of OCT-embedded sections, embryos were harvested at various ages, dissected and fixed in 1% PFA/PBS at 4°C overnight. Fixed embryos were then dehydrated gradually, first in 15% sucrose for 4-6 h at room temperature and then in 30% sucrose overnight at 4°C. Next, samples were dissected and soaked in 15% sucrose/50% OCT for 30-60 min and then embedded in OCT. Frozen samples were immediately sectioned at 10 µm and mounted onto slides.

Histological analysis and fluorescent *in situ* hybridization

Safranin-O/Fast Green staining was performed following standard protocols. Double fluorescent *in situ* hybridizations (dbFISH) on paraffin sections were performed using digoxigenin (DIG)- and fluorescein (FITC)-labeled probes (Shwartz and Zelzer, 2014). See Table S1 for probes. Probes were detected using anti-DIG-POD (Roche, 11207733910, 1:300) and anti-FITC-POD (Roche, 11207733910, 1:300), followed by Cy3- or Cy2-tyramide labeled fluorescent dyes, according to the instructions of the TSA Plus Fluorescent Systems Kit (PerkinElmer).

Immunofluorescence staining

For immunofluorescence staining for SOX9 and COL2A1, 7 µm thick paraffin sections of embryo limbs were deparaffinized and rehydrated in water. Antigen was then retrieved in 10 mM citrate buffer (pH 6.0), boiled and cooked for 10 min in a microwave oven. In order to block non-specific binding of immunoglobulin, sections were incubated with 7% goat serum, 1% bovine serum albumin dissolved in PBST (PBS+0.1% Triton X-100+0.01% sodium azide). Following blockage, sections were incubated overnight at 4°C with primary anti-SOX9 antibody (1:200, AB5535, Millipore). Then, sections were washed in PBST and incubated with Cy3-conjugated secondary fluorescent antibodies (1:100, 611-165-215, Jackson ImmunoResearch). After staining for SOX9, slides were washed in PBST and fixed in 4% PFA at room temperature for 10 min. Then, slides were incubated with proteinase K (Sigma-Aldrich, P9290), washed and post-fixed again in 4% PFA. Next, sections were washed and incubated overnight at 4°C with primary anti-COL2A1 antibody (1:50, II-II6B3, the Developmental Studies Hybridoma Bank). The next day, sections were washed in PBST and incubated with Cy2-conjugated secondary fluorescent antibodies (1:200, 615-222-214, Jackson ImmunoResearch). Occasionally, slides were counterstained using DAPI. Slides were mounted with Immu-mount aqueous-based mounting medium (Thermo Fisher Scientific).

For immunofluorescence staining for SOX9 and *ScxGFP*, 10 µm cryostat sections of embryo limbs endogenously labeled for *ScxGFP* were used. SOX9 immunofluorescence staining was performed as described above, using primary SOX9 antibody and secondary Cy3-fluorescent antibodies.

Acknowledgments

We thank N. Konstantin for expert editorial assistance and all other members of the Zelzer laboratory for their advice and suggestions. We thank R. Schweitzer for providing the *ScxGFP* mice, and H. Akiyama for providing the *Sox9-CreER^{T2}* mice. We thank H. Vega from the Weizmann Institute Department of Design, Photography and Printing for designing the model.

Competing interests

The authors declare no competing or financial interests.

Author contributions

Conceptualization: S.E., E.Z.; Methodology: S.E.; Validation: E.Z.; Investigation: S.E., S.R., S.K., L.L., E.Z.; Writing - original draft: S.E., E.Z.; Visualization: S.E., S.R., S.K.; Supervision: E.Z.; Project administration: E.Z.; Funding acquisition: E.Z.

Funding

This work was supported by grants from the United States-Israel Binational Science Foundation (BSF) [#2011122], the European Research Council (ERC) [#310098], and the Minerva Foundation [#711428].

Supplementary information

Supplementary information available online at
http://dev.biologists.org/lookup/doi/10.1242/dev.167452.supplemental

References

Abdala, V., Vera, M. C. and Ponssa, M. L. (2017). On the presence of the patella in frogs. *Anat. Rec.* **300**, 1747-1755.

Askary, A., Mork, L., Paul, S., He, X., Izuhara, A. K., Gopalakrishnan, S., Ichida, J. K., McMahon, A. P., Dabizljevic, S., Dale, R. et al. (2015). Iroquois proteins promote skeletal joint formation by maintaining chondrocytes in an immature state. *Dev. Cell* **35**, 358-365.

Bandyopadhyay, A., Tsuji, K., Cox, K., Harfe, B. D., Rosen, V. and Tabin, C. J. (2006). Genetic Analysis of the Roles of BMP2, BMP4, and BMP7 in Limb Patterning and Skeletogenesis. *PLoS Genet.* **2**, e216.

Bizarro, A. H. (1921). On sesamoid and supernumerary bones of the limbs. *J. Anat.* **55**, 256-268.

Blitz, E., Viukov, S., Sharir, A., Shwartz, Y., Galloway, J. L., Pryce, B. A., Johnson, R. L., Tabin, C. J., Schweitzer, R. and Zelzer, E. (2009). Bone ridge patterning during musculoskeletal assembly is mediated through SCX regulation of Bmp4 at the tendon-skeleton junction. *Dev. Cell* **17**, 861-873.

Blitz, E., Sharir, A., Akiyama, H. and Zelzer, E. (2013). Tendon-bone attachment unit is formed modularly by a distinct pool of Scx-and Sox9-positive progenitors. *Development* **140**, 2680-2690.

Carter, D. (1998). Epigenetic mechanical factors in the evolution of long bone epiphyses. *Zool. J. Linn. Soc.* **123**, 163-178.

Chytil, A., Magnuson, M. A., Wright, C. V. E. and Moses, H. L. (2002). Conditional inactivation of the TGF-β type II receptor using Cre: lox. *Genesis* **32**, 73-75.

Corina Vera, M., Laura Ponssa, M. and Abdala, V. (2015). Further data on sesamoid identity from two anuran species: morphology and development of anuran skeletal elements. *Anat. Rec.* **298**, 1376-1394.

Doherty, A. H., Lowder, E. M., Jacquet, R. D. and Landis, W. J. (2010). Murine metapodophalangeal sesamoid bones: morphology and potential means of

mineralization underlying function. *Anat. Rec.: Adv. Integr. Anat. Evol. Biol.* **293**, 775-785.
Eyal, S., Blitz, E., Shwartz, Y., Akiyama, H., Schweitzer, R. and Zelzer, E. (2015). On the development of the patella. *Development* **142**, 1831-1839.
Eyal, S., Kult, S., Rubin, S., Krief, S., Pineault, K. M., Wellik, D. and Zelzer, E. (2018). Bone morphology is regulated modularly by global and regional genetic programs. *bioRxiv*.
Gamer, L. W., Pregizer, S., Gamer, J., Feigenson, M., Ionescu, A., Li, Q., Han, L. and Rosen, V. (2018). The role of Bmp2 in the maturation and maintenance of the murine knee joint. *J. Bone Miner. Res.* **33**, 1708-1717.
Hall, B. K. (2005). *Bones and Cartilage: Developmental and Evolutionary Skeletal Biology*. Academic Press.
Hauser, N. H., Hoechel, S., Toranelli, M., Klaws, J. and Müller-Gerbl, M. (2015). Functional and structural details about the fabella: what the important stabilizer looks like in the Central European population. *BioMed Res. Int.* **2015**, 1-8.
Jerez, A., Mangione, S. and Abdala, V. (2009). Occurrence and distribution of sesamoid bones in squamates: a comparative approach. *Acta Zoo.* **91**, 295-305.
Jin, Z. W., Shibata, S., Abe, H., Jin, Y., Li, X. W. and Murakami, G. (2017). A new insight into the fabella at knee: the foetal development and evolution. *Folia Morphol.* **76**, 87-93.
Koyama, E., Yasuda, T., Minugh-Purvis, N., Kinumatsu, T., Yallowitz, A. R., Wellik, D. M. and Pacifici, M. (2010). Hox11 genes establish synovial joint organization and phylogenetic characteristics in developing mouse zeugopod skeletal elements. *Development* **137**, 3795-3800.
Lennox, I. A., Cobb, A. G., Knowles, J. and Bentley, G. (1994). Knee function after patellectomy. A 12-to 48-year follow-up. *Bone Joint J.* **76**, 485-487.
Liu, W., Selever, J., Wang, D., Lu, M.-F., Moses, K. A., Schwartz, R. J. and Martin, J. F. (2004). Bmp4 signaling is required for outflow-tract septation and branchial-arch artery remodeling. *Proc. Natl Acad. Sci. USA* **101**, 4489-4494.
Logan, M., Martin, J. F., Nagy, A., Lobe, C., Olson, E. N. and Tabin, C. J. (2002). Expression of Cre recombinase in the developing mouse limb bud driven by a Prxl enhancer. *Genesis* **33**, 77-80.
Ma, L. and Martin, J. F. (2005). Generation of a Bmp2 conditional null allele. *Genesis* **42**, 203-206.
Madisen, L., Zwingman, T. A., Sunkin, S. M., Oh, S. W., Zariwala, H. A., Gu, H., Ng, L. L., Palmiter, R. D., Hawrylycz, M. J., Jones, A. R. et al. (2010). A robust and high-throughput Cre reporting and characterization system for the whole mouse brain. *Nat. Neurosci.* **13**, 133-140.
Maisano, J. A. (2002). The potential utility of postnatal skeletal developmental patterns in squamate phylogenetics. *Zool. J. Linn. Soc.* **136**, 277-313.
McDonald, L. A., Gerrelli, D., Fok, Y., Hurst, L. D. and Tickle, C. (2010). Comparison of Iroquois gene expression in limbs/fins of vertebrate embryos: iroquois gene expression. *J. Anat.* **216**, 683-691.
Mottershead, S. (1988). Sesamoid bones and cartilages: an enquiry into their function. *Clin. Anat.* **1**, 59-62.
Pai, A. C. (1965). Developmental genetics of a lethal mutation, muscular dysgenesis (MDG), in the mouse: I. Genetic analysis and gross morphology. *Dev. Biol.* **11**, 82-92.
Parsons, F. G. (1904). Observations on traction epiphyses. *J. Anat. Physiol.* **38**, 248.
Parsons, F. G. (1908). Further remarks on traction epiphyses. *J. Anat. Physiol.* **42**, 388.
Pearson, K. and Davin, A. G. (1921a). On the sesamoids of the knee-joint. *Biometrika* **13**, 133.
Pearson, K. and Davin, A. G. (1921b). On the sesamoids of the knee-joint: part II. Evolution of the sesamoids. *Biometrika* **13**, 350.
Phukubye, P. and Oyedele, O. (2011). The incidence and structure of the fabella in a South African cadaver sample. *Clin. Anat.* **24**, 84-90.
Pignatti, E., Zeller, R. and Zuniga, A. (2014). To BMP or not to BMP during vertebrate limb bud development. *Semin. Cell Dev. Biol.* **32**, 119-127.
Ponssa, M. L., Goldberg, J. and Abdala, V. (2010). Sesamoids in anurans: new data, old issues. *Anat. Rec.: Adv. Integr. Anat. Evol. Biol.* **293**, 1646-1668.
Pryce, B. A., Brent, A. E., Murchison, N. D., Tabin, C. J. and Schweitzer, R. (2007). Generation of transgenic tendon reporters, ScxGFP and ScxAP, using regulatory elements of the scleraxis gene. *Dev. Dyn.* **236**, 1677-1682.
Samuels, M. E., Regnault, S. and Hutchinson, J. R. (2017). Evolution of the patellar sesamoid bone in mammals. *PeerJ* **5**, e3103.
Sarin, V. K., Erickson, G. M., Giori, N. J., Bergman, A. G. and Carter, D. R. (1999). Coincident development of sesamoid bones and clues to their evolution. *Anat. Rec.* **257**, 174-180.
Schindler, O. S. and Scott, W. N. (2011). Basic kinematics and biomechanics of the patello-femoral joint Part 1: the native patella. *Acta Orthop. Belg.* **77**, 421-431.
Selever, J., Liu, W., Lu, M.-F., Behringer, R. R. and Martin, J. F. (2004). Bmp4 in limb bud mesoderm regulates digit pattern by controlling AER development. *Dev. Biol.* **276**, 268-279.
Selleri, L., Depew, M. J., Jacobs, Y., Chanda, S. K., Tsang, K. Y., Cheah, K. S., Rubenstein, J. L., O'Gorman, S. and Cleary, M. L. (2001). Requirement for Pbx1 in skeletal patterning and programming chondrocyte proliferation and differentiation. *Development* **128**, 3543-3557.
Shwartz, Y. and Zelzer, E. (2014). Nonradioactive in situ hybridization on skeletal tissue sections. In *Skeletal Development and Repair. Methods in Molecular Biology*, **1130** (ed. M. Hilton), pp. 203-215. Humana Press.
Soeda, T., Deng, J. M., de Crombrugghe, B., Behringer, R. R., Nakamura, T. and Akiyama, H. (2010). Sox9-expressing precursors are the cellular origin of the cruciate ligament of the knee joint and the limb tendons. *Genesis* **48**, 635-644.
Sugimoto, Y., Takimoto, A., Akiyama, H., Kist, R., Scherer, G., Nakamura, T., Hiraki, Y. and Shukunami, C. (2013). Scx+/Sox9+ progenitors contribute to the establishment of the junction between cartilage and tendon/ligament. *Development* **140**, 2280-2288.
Sutton, F., Thompson, C., Lipke, J. and Kettelkamp, D. (1976). The effect of patellectomy on knee function. *J. Bone Joint Surg.* **58**, 537-540.
Vickaryous, M. K. and Olson, W. M. (2007). Sesamoids and ossicles in the appendicular skeleton. In *Fins into Limbs: Evolution, Development, and Transformation* (ed. B.K. Hall), pp. 323-341. University of Chicago Press.
Wirtschafter, Z. T. and Tsujimura, J. K. (1961). The sesamoid bones in the C3H mouse. *Anat. Rec.* **139**, 399-408.

Table S1. In situ hybridization RNA antisense probes

RNA Probe Name	Genomic Position	Ref-Seq accession	Size
Sox9	50-797	NM_011448.4	747bp
Scleraxis	Full length	NM_198885.3	964bp
Tenomodulin	654-1299	NM_022322.2	645bp
Gdf5	1-1437	NM_008109.3	1436bp
Tppp3	149-680	NM_026481.3	531bp
Irx1	503-1109	NM_010573.2	606bp